The Journal of the Acoustical Society of America

OCTOBER 29 2026

Modeling the effects of seasonal weather on rocket launch-ascent sonic boom footprints in Southern California

Mark C. Anderson ; Kent L. Gee ; Lucas K. Hall

Check for updates

J. Acoust. Soc. Am. 160, 3572–3582 (2026)
https://doi.org/10.1121/10.0046863

View Online Export Citation

Articles You May Be Interested In

Weather Balloon Ascent Rate
Phys. Teach. (May 2016)

Investigation of deturbing methods for sonic boom signatures
J. Acoust. Soc. Am. (March 2018)

An infrasound source analysis of the OSIRIS-REx sample return capsule hypersonic re-entry
J. Acoust. Soc. Am. (December 2025)

02 November 2026 18:49:36



ASA ACOUSTICAL SOCIETY OF AMERICA

JASA ARTICLE

Modeling the effects of seasonal weather on rocket launch-ascent sonic boom footprints in Southern California

Mark C. Anderson,[1,a] Kent L. Gee,[1] and Lucas K. Hall[2]
[1]Department of Physics and Astronomy, Brigham Young University, Provo, Utah 84602, USA
[2]Department of Biology, California State University Bakersfield, Bakersfield, California 93311, USA

ABSTRACT:
When rockets ascend, accelerate, and pitch over toward orbit, they can generate sonic booms audible on the ground over 100 km from the launch site, as observed with recent launches from Vandenberg Space Force Base. The locations where these booms arrive vary seasonally, with some areas experiencing them only at certain times of year. In this paper, the seasonal variation is explored and modeled using PCBOOM 7.5.0, with simulations run using measured and modeled weather profiles from 2020 to 2025. PCBOOM peak overpressure footprints were interpolated to four locations where sonic booms have been reported and measured: Carpinteria, Ojai, Ventura, and Oxnard. The probability of a sonic boom occurring at each location was higher in the winter and lower in the summer (all seasons defined in the northern hemisphere). Changes in the footprint location were linked to seasonal changes in weather. Specifically, the changes in upper-level winds (stratospheric and mesospheric) influenced large changes in the land area that received a sonic boom. Strategic seasonal launch scheduling for missions should be considered to enable launches along all azimuths while minimizing the occurrence of sonic booms on land. © *2026 Acoustical Society of America*. https://doi.org/10.1121/10.0046863

(Received 15 April 2026; revised 18 August 2026; accepted 22 September 2026; published online 29 October 2026)

[Editor: Didier Dragna] Pages: 3572–3582

02 November 2026 18:49:36

I. INTRODUCTION

As a rocket ascends through the atmosphere at supersonic speeds, it produces a sonic boom. Although a strictly vertical trajectory produces an upward-propagating sonic boom, an orbital rocket must pitch over as it ascends so that it reaches the necessary horizontal velocity required for orbit. This pitching over, along with the vehicle's acceleration, produces a sonic boom that intersects the surface below (Glatt *et al.*, 1975). Such sonic booms were measured in the Atlantic Ocean during Saturn V launches[1] (Hilton *et al.*, 1972; Henderson and Hilton, 1974a, 1974b; Hilton and Henderson, 1974) and Space Shuttle launches (Garcia *et al.*, 1983; Stansbery *et al.*, 1983; Stansbery and Stanley, 1984; Stansbery, 1985; Stanley, 1984; Maglieri *et al.*, 2011). Additional measurements have been made of the Titan IV (Stewart, 1993; Francine and Stewart, 1995; Downing and Plotkin, 1996) and the Atlas V (Ortt, 2015). However, almost all previous studies have focused on measuring the sonic boom out at sea or on islands (Haber, 1981; Wooten, 1983; Stewart, 1993; Ortt, 2015). Previous studies have also been focused either on the boom centerline or along the boom focus line, and little research has been done outside these regions.

The highest-amplitude portion of the rocket sonic boom footprint is typically the leading edge, where one or more focus booms can occur. Focus booms are the result of multiple sound rays arriving simultaneously and combining to produce a higher overpressure than elsewhere in the footprint (Maglieri *et al.*, 2014). For example, the peak overpressures in the Saturn V focus region were measured as high as 8.9 pounds per square foot (psf) (Henderson and Hilton, 1974b), with 6.8 psf for the Space Shuttle (Maglieri *et al.*, 2011). Away from the focus, the pressures rapidly drop to ∼1–3 psf and continue to decrease with distance both downrange and laterally.

For southeasterly launches from Vandenberg Space Force Base (VSFB), the sonic boom footprint (including the focus booms) can intercept the areas along the coast of California, like Ventura County (Gee *et al.*, 2026). Although sonic booms measured during the summer months of 2024 tended to be mild and of low amplitude, continued measurements indicated a strong seasonal trend in the sonic boom intensity and footprint locations on land (Kellison *et al.* 2025; Bickmore *et al.*, 2025), with the sonic boom being audible in certain locations only during parts of the year. Conversations with local individuals substantiated the notion that both the sonic boom occurrence and intensity are seasonal. This led to the hypothesis that seasonal weather variation could explain the seasonal variability in the sonic booms on land. This hypothesis is tested in this paper.

The purpose of this paper is to determine whether seasonal weather variation can explain the observed changes in the sonic boom footprints observed in Southern California. The computational model and weather profile data are discussed in Sec. II. The model's outputs are then compared to measured data in Sec. III. Section IV is focused on modeling a single launch trajectory for each day of 2020–2025 and investigating the seasonal trends at four locations. In Sec. V, the upper-level winds are shown to control the modeled

[a]Email: mark.anderson@byu.net

 © 2026 Acoustical Society of America

https://doi.org/10.1121/10.0046863

footprint location in different seasons. Section VI then proposes a possible solution for sonic boom mitigation on land that would allow for all azimuths to be used for launches, referred to as strategic seasonal launch scheduling (SSLS). Conclusions are then presented in Sec. VII.

II. METHODS

A. PCBOOM

NASA's PCBOOM 7.5.0 software (Lonzaga *et al.*, 2025a,b) was used in this study to estimate sonic boom footprint locations and signature overpressures. PCBOOM is a software package that combines acoustic ray tracing and nonlinear acoustic propagation to predict footprints, waveform shapes, and metrics for sonic booms. Although it has primarily been validated for traditional supersonic aircraft, it has been used for rocket ascent sonic booms in the past (Downing and Plotkin, 1996) and other high-altitude hypersonic vehicle modeling. For example, an earlier version (PCBOOM 4) accurately predicted the overpressure and arrival time of a small reentry capsule (Plotkin *et al.*, 2006). In this paper, PCBOOM was run in the Carlson Launch mode, which uses the work of Tiegerman (1975) to estimate the sonic boom source function. The methods of Tiegerman (1975) use the drag to estimate sonic booms from hypersonic vehicles and continues to be used in modern spacecraft reentry modeling (Bishop *et al.*, 2025). The time-varying weight and thrust were input in the trajectory data, the plume drag was estimated as 20% of the thrust, and a shape factor curve number (IUN) of 13 was assumed, all following recommendations from the PCBOOM user's manual for a Titan rocket (Lonzaga *et al.*, 2025a). Because of known software instability when using the enhanced Burgers solver for orbital rocket launches, the lossless solver was used instead assuming that the footprint shape was unaffected by the choice of waveform solver and that the fine waveform details, like rise time, are not especially important to the present study. The lack of absorption effects is one of the reasons that discussions in this paper are limited to peak overpressure, and frequency-dependent sonic boom perception metrics (Loubeau and Page, 2018) are not included here.

A second reason that only the peak overpressure is considered in this paper is that PCBOOM is currently unable to accurately predict the full waveform using its built-in source model for an ascending rocket. PCBOOM creates an equivalent N-wave F-function for the vehicle body and then immediately follows it with an F-function for the plume using "a combination of Tiegerman's hypersonic blunt body model and Carlson's equivalent N-wave" (Lonzaga, 2025a) where "[t]he Carlson parameters are based on a shape factor corresponding to Tiegerman's hypersonic boom theory with drag corresponding to the engine's plume drag, and length from the Jarvinen-Hill universal plume model" (Lonzaga, 2025b). Inspection of the output files for the analyses in this paper indicates that the predicted waveforms on the ground are typically N-waves with durations less than one second.[2] However, such ground waveforms are inconsistent with measurements, where rocket ascent sonic booms tend to be shaped like blast waves, with an overpressure followed by a gradual rarefaction and return to ambient conditions, lasting several seconds (Hilton *et al.*, 1972; Henderson and Hilton, 1974a,b; Hilton and Henderson, 1974; Stansbery, 1985; Francine and Stewart, 1995; Gee *et al.*, 2026). Before rigorous waveform and spectral comparisons with measurements can be made, an improved source model that accounts for the dominating effects and indefinite length of the plume needs to be implemented. For the purposes of this paper, which is intended to show trends in footprint location and rough overpressure magnitudes, using the overpressure alone is sufficient.

Preliminary simulations indicate that the sonic booms reaching the ground in the study area were emitted around 25–65 km in altitude, with the focus booms being emitted near the lower end of this range. Therefore, it is important to obtain corresponding weather profiles over this full range. This is the topic of Sec. II B.

B. Weather data

Sample weather profile data are shown in Fig. 1. The variables used by PCBOOM are the (a) temperature, (b) zonal wind, (c) meridional wind, (d) relative humidity, and (e) pressure. Multiple sources were used to produce the profiles.[3] At low altitudes (0 to ∼30 km), weather balloon data were used from the Integrated Global Radiosonde Archive (IGRA) (Durre *et al.*, 2006). These balloons were nominally launched twice daily from VSFB. At medium altitudes (∼30 to ∼48 km), the European Centre for Medium-Range Weather Forecasts (ECMWF) Reanalysis v5 (ERA5) model was used [Hersbach *et al.*, 2023; Copernicus Climate Change Service (CCCS), 2023]. Although the ERA5 profiles were calculated over Santa Rosa Island (undertrack of the rocket), the ERA5 values at low altitudes agreed well with the radiosonde data from VSFB, demonstrating that the ERA5 data are a reliable proxy for measured profiles. Additionally, this substantiates the assumption that within the study region, the weather data can be assumed range independent. At high altitudes above the ERA5 simulations (∼48–70 km), a range reference atmosphere for each month was used for the wind components (Boire *et al.*, 1983; see Appendix), whereas a 1976 standard atmosphere was used for the temperature and pressure [National Oceanic and Atmospheric Administration (NOAA), 1976]. To reduce steep gradients occurring when the top point of the ERA5 simulation does not match the high-altitude reference or standard atmosphere, the high-altitude atmospheric data begin at 55 km, and the values between ∼48 and 55 km are linearly interpolated. Although it is possible to investigate multiple models and methods for constructing the full weather profiles, it is worth noting that Anderson and Gee (2025) and Lympany *et al.* (2025) presented independent studies of weather effects on rocket ascent sonic boom footprints where each used different weather data sources. Anderson and Gee (2025) used only the IGRA weather balloon data, whereas Lympany *et al.* (2025) used the NASA

02 November 2026 18:49:36

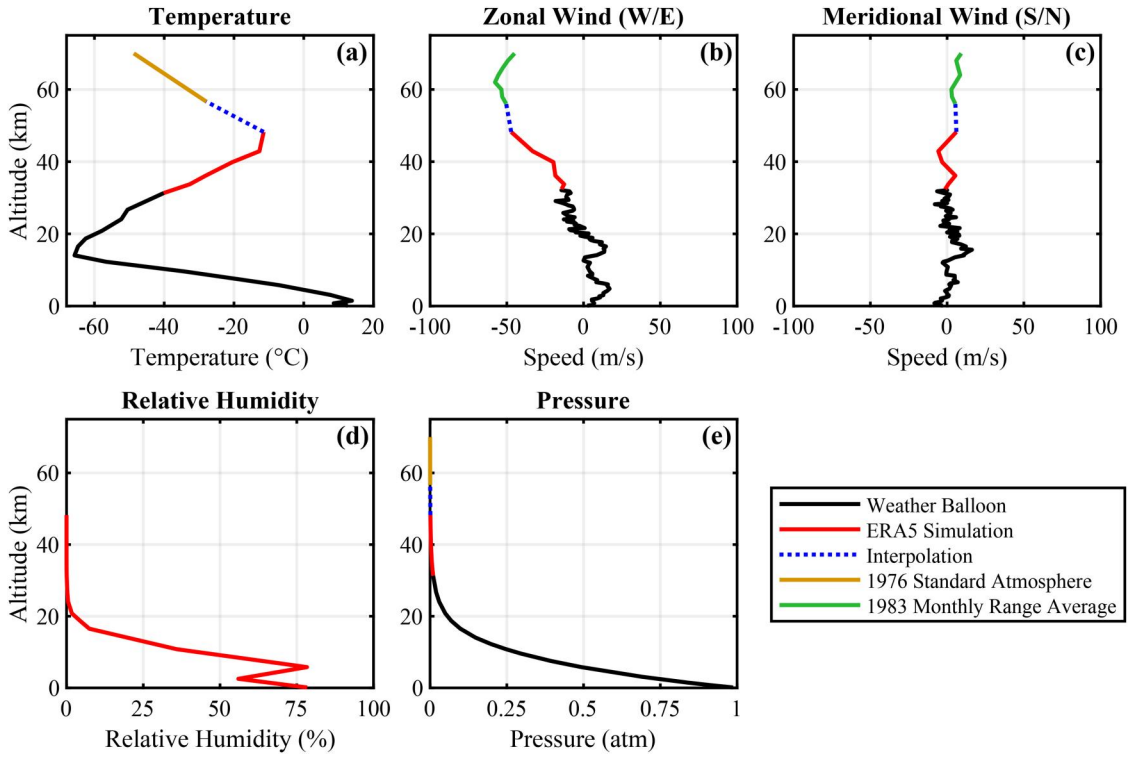


FIG. 1. Example weather profiles (19 June 2023). The five variables considered in the simulations are the (a) temperature, (b) zonal wind (west-blowing is negative, east-blowing is positive), (c) meridional wind (south-blowing is negative, north-blowing is positive), (d) relative humidity, and (e) pressure. Values are colored according to data source.

Horizontal Wind Model 2014 (Drob *et al.*, 2015). The trends and conclusions agreed with each other and with those found in this paper. Although different weather models should be investigated in the future, the conclusions in this paper are not expected to be especially sensitive to model choice. Additionally, the trends observed in this paper were independent of whether the data at 0000 UTC or 1200 UTC were used. However, because the 0000 UTC data had large gaps between October 2021 and October 2022, only the 1200 UTC data are used throughout the remainder of this paper, except where appropriate in Sec. III. Because trends in this paper were independent of balloon time, it is assumed that the same overall trends hold regardless of rocket launch time.

III. COMPARISON WITH MEASURED DATA

To determine whether the PCBOOM results are reliable for this use case, it is necessary to first demonstrate the degree to which the PCBOOM simulations agree with measured data. Contributing to this comparison, acoustic measurements were performed beginning in June 2024 (Kellison *et al.*, 2025; Gee *et al.*, 2026) and continued through 2025 (Bickmore *et al.*, 2025). Although full results have not yet been published, a subset of the measured data is shown in Fig. 2 for comparison with simulations. The simulations were all performed using a single Starlink Group 9 first-stage trajectory (terminating at engine cutoff) provided by VSFB, which is also similar to the Starlink Group 11 trajectory. The only differences between the simulations are the weather profiles, where the closest weather profile in time for each launch (either before or after) was used for each simulation. The launches considered are the Starlink 9-3 (July 12, 2024), Starlink 9-4 (July 28, 2024), Starlink 11-2 (December 14, 2024), and Starlink 11-11 (April 8, 2025) missions. As expected, based on previous measurements (Hilton *et al.*, 1972; Henderson and Hilton, 1974a,b), the pressures at the start of the footprint (northwest) are highest, and the pressures tend to decrease with distance from this high-pressure "focus" region, although the pressure decreases through the footprint are not monotonic when atmospheric effects are taken into account as shown in Fig. 2. Also, the simulated results show the same trends in footprint origin. It is worth noting that although the analyses in this paper are limited to the sonic boom produced during the first stage phase of flight, a sonic boom is still expected to be produced by the second stage. This second stage sonic boom would continue the footprint toward the southeast, gradually decreasing in amplitude as the rocket ascends to higher altitudes.

The similarity between the PCBOOM simulations and the measurements provides some confidence in the use of PCBOOM for the remainder of this paper. That is, the footprint leading edge and overpressures throughout are similar between PCBOOM and measurements. Because of the source model issues raised in Sec. II A, a rigorous comparison of overpressure amplitudes is not directly considered in this paper. For Starlink 9-3, few booms were measured on land, and those that were measured had low overpressures, typically below 0.1 psf. This was mirrored by the simulations,

02 November 2026 18:49:36

https://doi.org/10.1121/10.0046863

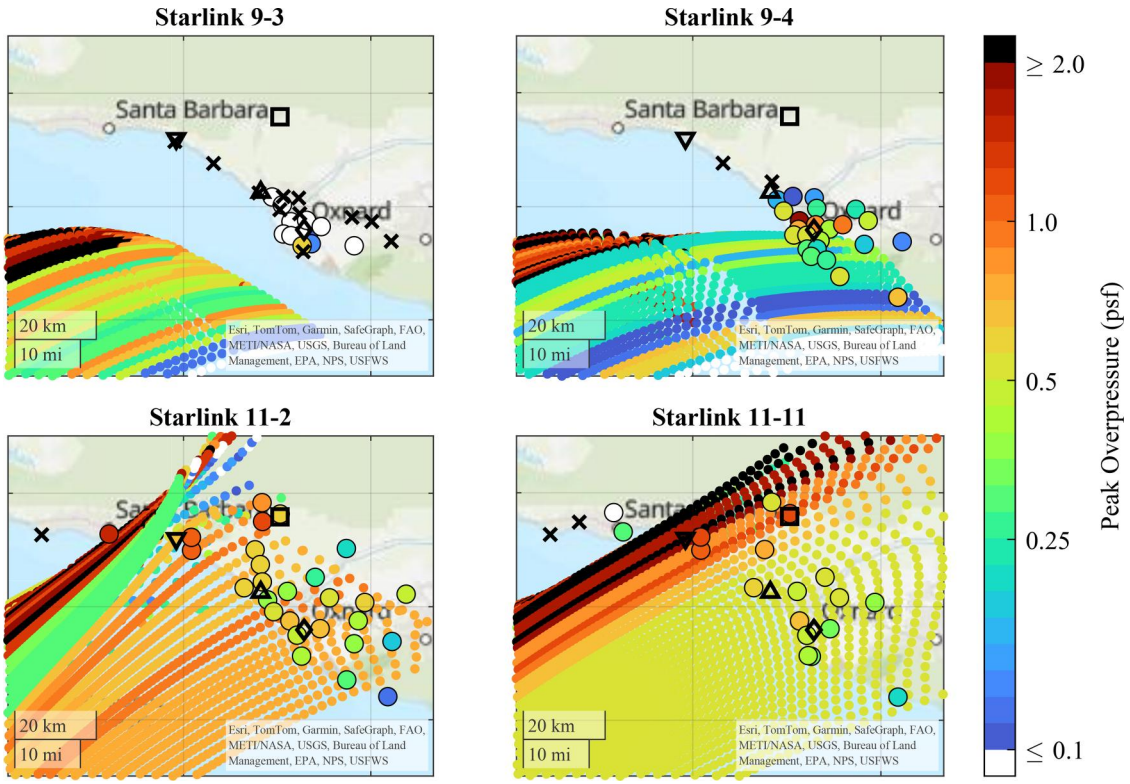


FIG. 2. Demonstration that PCBOOM simulations can approximate the overall footprint behavior for four launches including the Starlink 9-3 (July 12, 2024), Starlink 9-4 (July 28, 2024), Starlink 11-2 (December 14, 2024), and Starlink 11-11 (April 8, 2025) missions. PCBOOM simulation results are indicated by small circles, and the measured results are indicated by the larger circles with black borders. Locations where measurements were performed but no boom was observed are indicated by a black ×. Also, included for later convenience are markers for the locations: Carpinteria (▽), Ojai (□), Ventura (△), Oxnard (◇). Esri, Environmental Systems Research Institute; FAO, Food and Agriculture Organization of the United Nations; METI, Ministry of Economy, Trade, and Industry; USGS, U.S. Geological Survey; EPA, Environmental Protection Agency; NPS, National Park Service; USFWS, U.S. Fish and Wildlife Service.

02 November 2026 18:49:36

which predicted that the footprint terminated offshore. In reality, a region outside the predicted sonic boom footprint is expected to receive low-amplitude acoustic waves (Maglieri *et al.*, 2014), explaining why such low-amplitude signatures could still be recorded outside the primary carpet. The Starlink 9-4 launch, which occurred only 16 days after the Starlink 9-3 launch, created sonic booms over more land area, and this is reflected in the simulations. The Starlink 11-2 launch produced a substantially different footprint on land. Sonic booms were measured as far north as Ojai and as far west as Santa Barbara, a change that is predicted by the simulation. Last, the Starlink 11-11 simulation indicates that the focus should again pass through the northern portion of the study area, which aligns with the highest overpressures in the measurements. Thus, it is concluded that PCBOOM 7.5.0, when coupled with proper weather data, can approximate the trends in measured footprint locations.

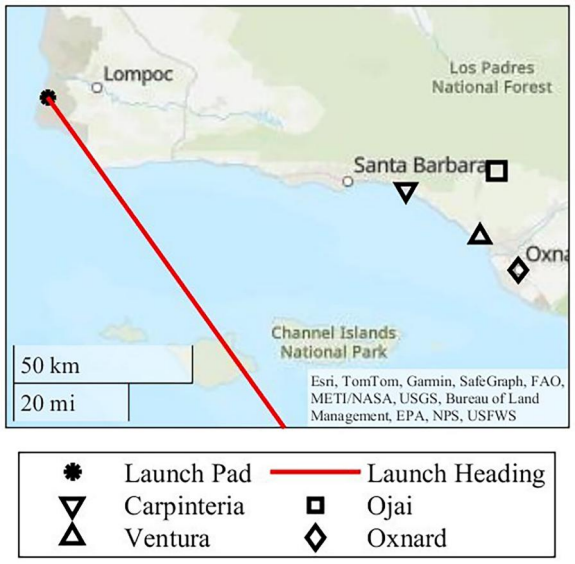


FIG. 3. The selected locations for further analysis along with the launch location and a 144° trajectory ground track representative of the trajectory used in this study. Esri, Environmental Systems Research Institute; FAO, Food and Agriculture Organization of the United Nations; METI, Ministry of Economy, Trade, and Industry; USGS, U.S. Geological Survey; EPA, Environmental Protection Agency; NPS, National Park Service; USFWS, U.S. Fish and Wildlife Service.

IV. FOOTPRINT MODELING BETWEEN 2020 AND 2025

To assess the effects of seasonal weather patterns on the sonic boom footprint, the same Starlink Group 9 trajectory was used to simulate flights with weather profiles taken from nearly every day of 2020–2025, only missing days

where the weather balloon data could not be obtained. The trajectory contains only the first-stage portion of flight and terminates at first-stage engine cutoff on ascent. The Starlink Group 9 trajectory has a launch heading of 144°, which makes it one of the closest launch trajectories to the coast. Only this trajectory is investigated in this paper because it has been found in continued measurements of the type shown in Gee *et al.* (2026) that as the trajectory moves farther from the coast, the sonic boom overpressures on land tend to decrease. For southerly trajectories, either no or very weak sonic booms are measured on land regardless of the season. Therefore, because the Starlink Group 9 trajectory represents the type of trajectory that is most likely to cause higher-overpressure sonic booms over more land area, it is the sole focus of the following analysis.

Once footprints were generated, the peak overpressures were interpolated using natural neighbor interpolation to four locations within the study area: Carpinteria, Ojai, Ventura, and Oxnard, shown in Figs. 2 and 3. The peak overpressure results are shown in Fig. 4 as a function of day. The reader is cautioned that although there is a correlation between sonic boom peak overpressure and sonic boom perception (Naka, 2013), there are other metrics that are better correlated (Naka, 2013; Loubeau *et al.*, 2015). Other than overpressure, a key factor in determining sonic boom perception is the shock rise time (Loubeau and Page, 2018; Shepherd and Sullivan, 1991). Thus, the overpressure results shown in this paper should not be taken to directly indicate sonic boom perception, and future analyses need to be performed to determine the perception of launch-ascent sonic booms. Anecdotally, pressures around 1 psf tend to be clearly audible outdoors, and higher pressures even more so. Lower pressures are also typically audible but can become decreasingly audible as the pressure drops. The three northernmost locations (Carpinteria, Ojai, and Ventura) show strong seasonality, tending to have almost no booms in the summer months (defined as May to September), although having some of the highest-amplitude booms in the winter months (defined as October to April). This result can be explained because these locations are on the northern edge of the footprint and so tend to receive no boom (outside the footprint) or are near the focus boom (barely inside the footprint). The southernmost location (Oxnard) also shows seasonality in peak overpressure, although it is not quite as prominent as at the northern locations. Additionally, the only value exceeding the axis limits in Fig. 4 is on

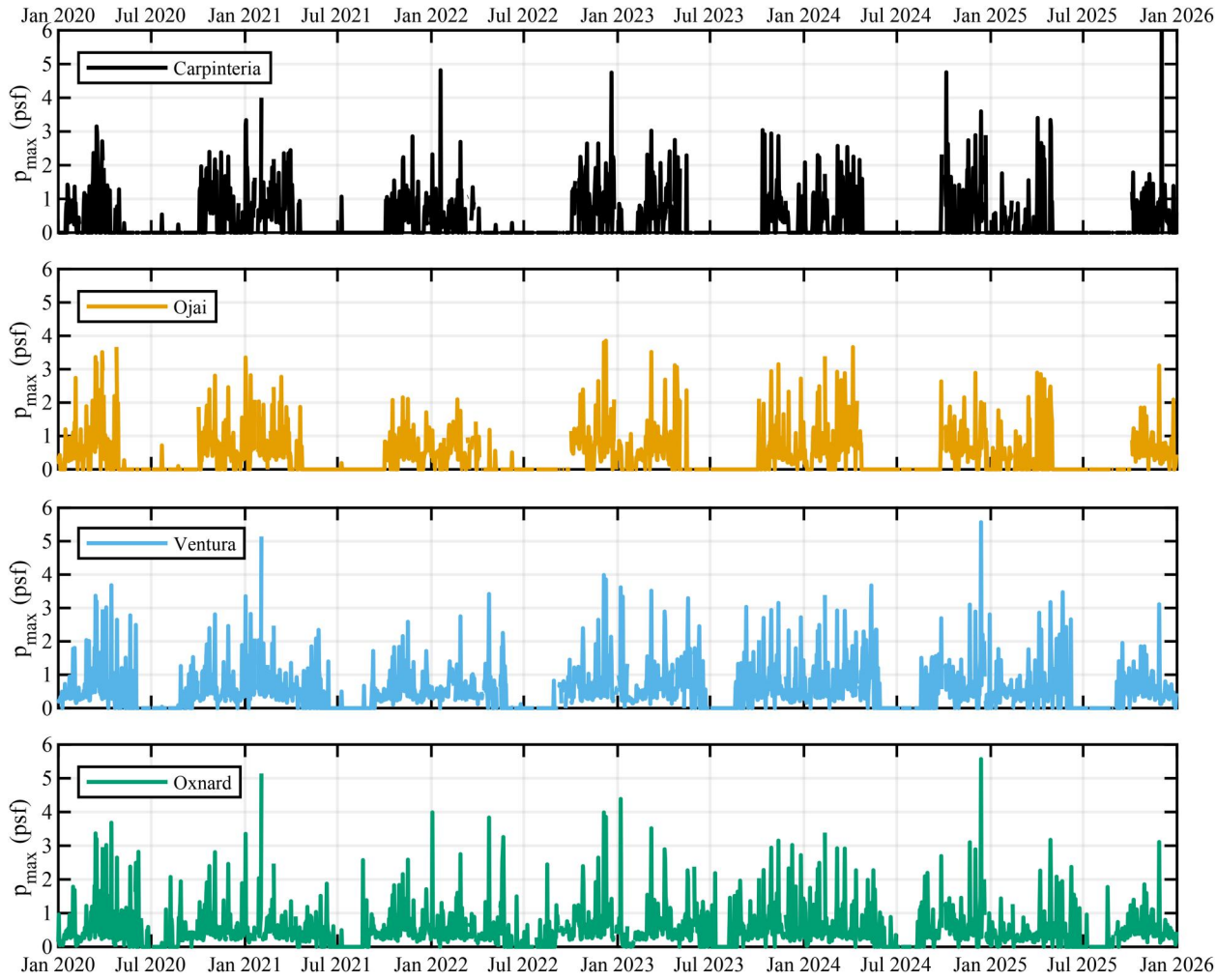


FIG. 4. Simulated overpressure predictions at each of the four locations. PCBOOM footprints from each day were interpolated to each location.

02 November 2026 18:49:36

https://doi.org/10.1121/10.0046863

December 12, 2025, for Carpinteria, with an overpressure of 7.2 psf. Although all the overpressures higher than 4 psf were inspected and found to be valid interpolations, only one (Carpinteria, January 19, 2022) was found to result from a convex footprint shape that may have exaggerated the overpressure.

To simplify the visualization of seasonal trends, the data in Fig. 4 were used to produce Fig. 5. To produce these results, the simulations in Fig. 4 were aggregated by month. Figure 5(a) shows the percentage of days in each month where PCBOOM (with the corresponding weather conditions) predicts a boom at each location. Although Ventura and Oxnard consistently have higher overall boom percentages, all four locations had lower percentages (dropping below 20%) at some time during the summer months and higher percentages (rising above 70%) at some time during the winter months. However, because Fig. 5(a) only considers whether a simulated boom of any amplitude occurred at each location, it is useful to consider also the median boom overpressures for each month, shown in Fig. 5(b). Days where booms are not predicted at a given location have overpressures of zero. The same trends are

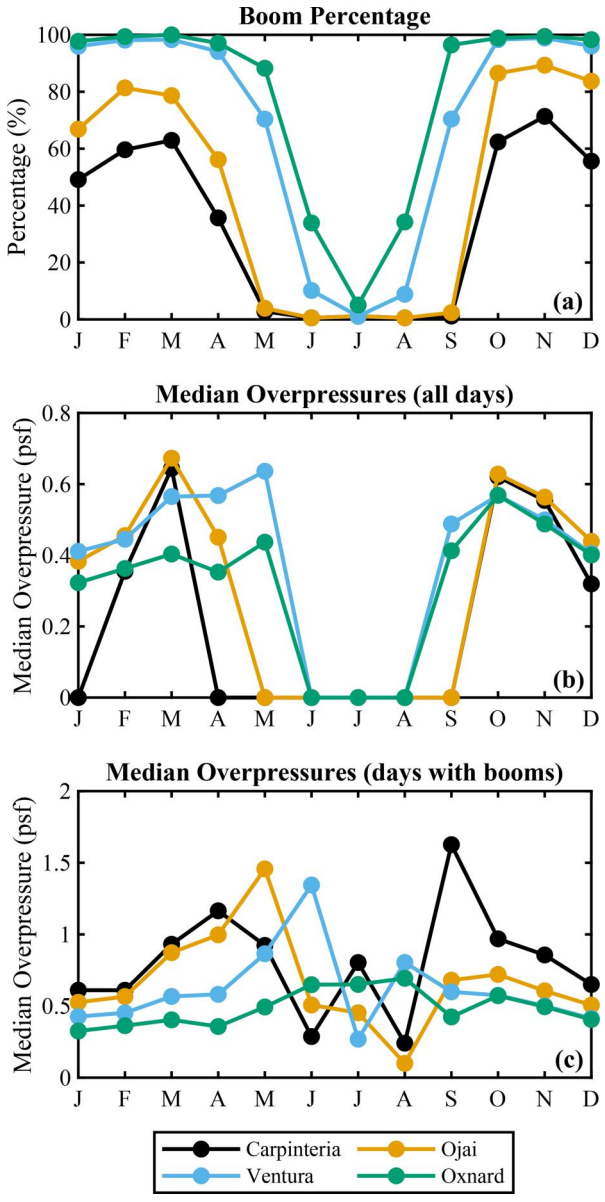


FIG. 5. Seasonal variation in sonic booms at each location of interest. (a) The percentage of days in each month where a sonic boom occurs at each location; (b) the median overpressures for each month, with no-boom days included as 0 psf; and (c) the median overpressures for each month, but with no-boom days discarded. J, January; F, February; M, March; A, April; M, May; J, June; J, July; A, August; S, September; O, October; N, November; D, December.

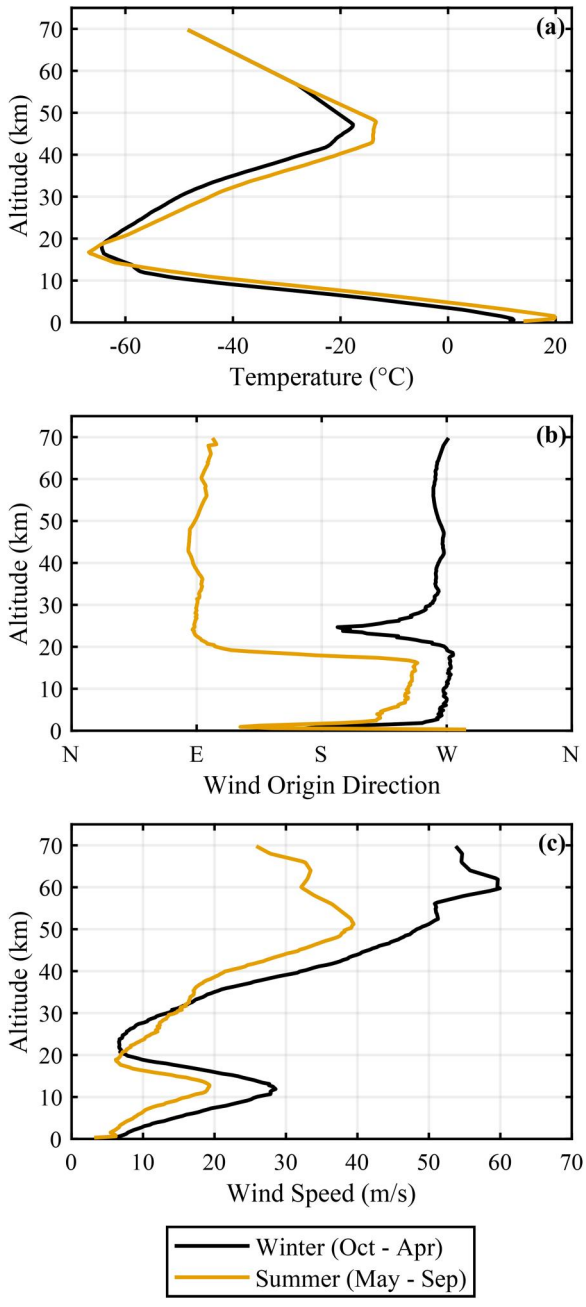


FIG. 6. The meteorological factors expected to predominantly shape the footprint. Median profiles are shown for two time periods: winter (October–April) and summer (May–September). The variables considered are the (a) temperature, (b) wind direction (defined as the direction from which the wind originates), and (c) wind speed.

02 November 2026 18:49:36

again visible, with median overpressures dropping to 0 psf in the summer months and rising above 0.5 psf at some point in the winter months. Last, although Fig. 5(b) shows the median values including days without booms predicted at each location, Fig. 5(c) shows the median overpressures including only those days where booms are predicted to occur for each given location. In this result, seasonal variation in overpressure is location-dependent, with less variation at the southernmost location (Oxnard, 0.3–0.7 psf) and more at the northernmost location (Carpinteria, 0.2–1.6 psf).

V. ASSESSING METEOROLOGICAL FACTORS

There are only five meteorological inputs to PCBOOM for describing the stratified atmosphere up to flight altitude: temperature, wind (zonal and meridional components), pressure, and relative humidity. Of these, only the temperature and wind (which can both strongly affect the local sound speed) are anticipated to play a dominant role in the ray tracing that determines the final footprint location. These variables are considered in Fig. 6, showing the median profiles across the entire study period for the seven winter (October–April) and the five summer (May–September) months. These time periods were chosen based on the trends observed in Fig. 5. Although the median temperature profiles appear similar for the two seasons, the upper-level (stratospheric and mesospheric) winds (>15 km) come from different directions, and the upper-level wind speed profiles gradually diverge. In the winter months, these winds mostly travel from the west toward land. In the summer months, the winds travel from the east toward the ocean. Because the largest relative differences in weather profiles occur for the wind direction, where there is almost a complete reversal of direction above 40 km, the following analysis focuses on how the upper-level wind direction affects the footprints.

To study the possible effects of upper-level wind direction on the sonic boom footprint, PCBOOM simulations were performed using eight different wind direction profiles, shown in Fig. 7(a). This study isolates the effects of upper-level wind direction and determines whether the upper-level wind differences in the winter (westerly/east-blowing winds) and summer (easterly/west-blowing winds) can account for the observed seasonal trends in footprint location. Below 15 km, the wind direction profiles all converge to the median wind direction across the entire multiyear simulation period, and above 15 km they separate into eight different directions. For all simulations, the median wind speed profile across the full multiyear simulation period was used and is shown in Fig. 7(b). Similarly, the temperature, pressure, and relative humidity profiles used here are the median profiles across the full multiyear simulation. Because the real-world upper-level winds in this region tend to have a strong zonal component (see the Appendix), the simulations with easterly or westerly wind components [(northeast, east, southeast, southwest, west, and northwest)] are expected to be more physical, whereas the purely northerly and southerly wind directions are included for completeness.

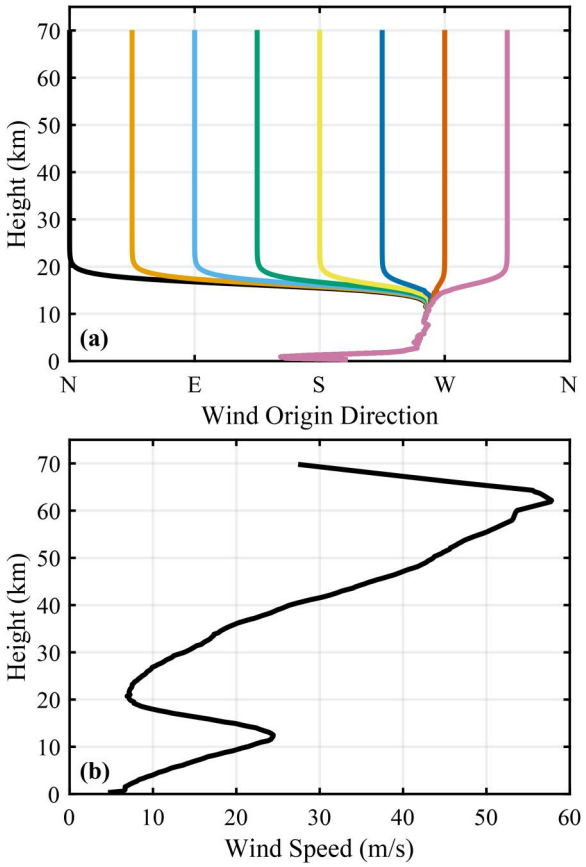


FIG. 7. Wind profiles used in the PCBOOM wind effects analysis. (a) The wind direction as a function of height. Values above 15 km are coerced to particular directions, whereas values at lower altitudes correspond to the median taken over the full range of dates in the multiyear simulations. (b) The median wind speed as a function of height over the full range of dates in the multiyear simulations.

The simulation results are shown in Fig. 8. Each subplot corresponds to the upper-level wind coming from a particular direction, and an arrow is included in each subplot to further clarify the wind vector. Locations corresponding to those in Figs. 3–5 are indicated. The overpressures are not included because it was found that small changes in how the atmosphere was defined caused large changes in overpressures for each wind condition, making interpretation of such overpressures less reliable. Meanwhile, the footprint shapes were resilient to these small changes in atmospheric definition, indicating that the footprint shapes are more reliably interpretable. Because the footprint shape is of primary interest here, the footprints are shown in a uniform gray color with the upper 20th percentile of overpressures colored in red to give an idea of where the focus region is. When the upper-level winds originate from the north, northeast, east, or southeast, there is an eastern lateral cutoff to the sonic boom footprint on land within the axis limits. However, when the upper-level winds originate from any of the other directions (south, southwest, west, or northwest),

02 November 2026 18:49:36

https://doi.org/10.1121/10.0046863

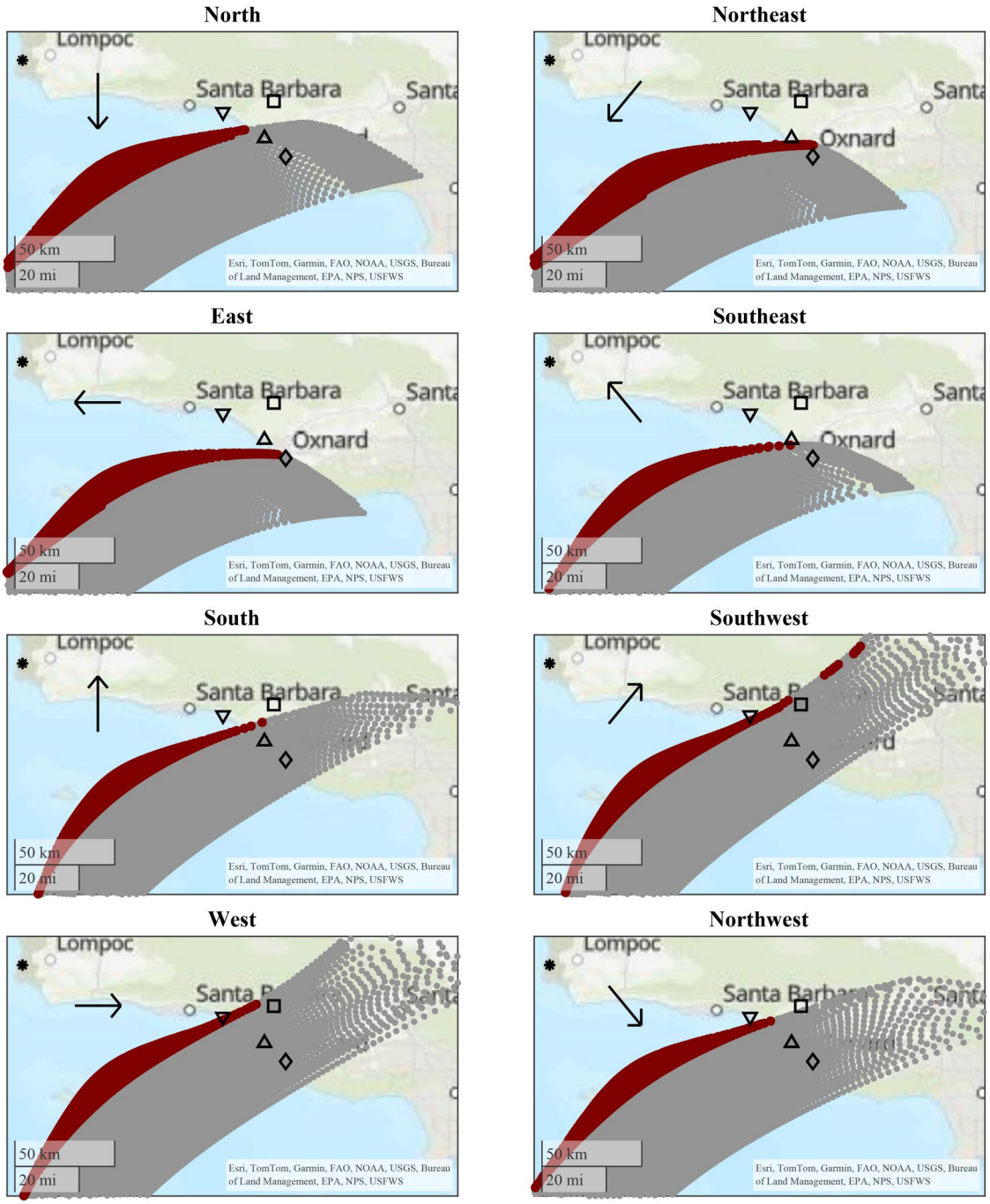


FIG. 8. The effects of upper-level (>15 km) wind direction on the sonic boom footprints. Locations of interest include Carpinteria (▽), Ojai (□), Ventura (△), Oxnard (◇), and the launch site (∗). Upper-level wind direction vectors are indicated on each subplot by an arrow. The titles indicate the direction from which the upper-level winds originate. To keep the emphasis on footprint locations, the upper 20th percentile of pressure values is colored in red, and the rest are colored in a uniform gray.

the eastern lateral cutoff is much farther inland. In fact, for the southwesterly and westerly wind cases, the footprint reaches as far inland as Lancaster, CA, and even into the Mojave Desert. The westerly winds also tend to produce a footprint that places Carpinteria and Ojai on the northern edge of the footprint, making it clear that these locations are at a higher probability of experiencing a focus boom when the upper-level winds blow from any of the westerly directions. These results validate the claim that changes in upper-level wind direction can explain the seasonal variation observed in measurements.

VI. STRATEGIC SEASONAL LAUNCH SCHEDULING (SSLS)

With the connection made between seasonal weather and sonic booms on land, it is possible to discuss a potential mitigation solution, referred to here as SSLS. The goal is to enable

02 November 2026 18:49:36

launch providers to launch all missions while simultaneously reducing the sonic boom footprints on land. If launch schedules can be flexible, then SSLS is a promising path forward.

SSLS at VSFB would operate on the principle that coastal trajectories in winter months (October–April) tend to produce higher-amplitude sonic booms over relatively large land areas, whereas the same trajectories in summer months (May–September) produce sonic booms that cover less land area and typically have lower amplitudes on land. For example, the probability of receiving a sonic boom in Ojai for a given launch along this 144° trajectory on a random day in the summer months is modeled to be less than 10%, whereas the probability for a launch in the winter months is modeled to be over 60% and even as high as 90% depending on the month (see Fig. 5). Meanwhile, ongoing measurements like those of Gee *et al.* (2026) indicate that southerly launch trajectories do not produce high-amplitude sonic booms on land regardless of the season. Although launch headings are typically set by the desired orbit for the payload, launches to low Earth orbit tend to be possible year-round. For example, launches along the 144° and other more-southerly headings from VSFB have happened throughout the different times of year. This suggests that there may be flexibility in scheduling launches for such low Earth orbit missions, which constitute the bulk of launches from VSFB today. Therefore, it is proposed that coastal launches be scheduled primarily for the summertime, when they produce weaker sonic booms on land, and the launches farther from the coast be launched in the wintertime, which also produces no (or weak) sonic booms on land. Following this pattern where possible could enable launch providers to launch all their planned missions throughout the year while reducing the sonic boom footprints on land.

A full study of different trajectories (including additional headings) throughout different seasons is required before recommendations for implementing SSLS can be concretely given. This paper provides a framework for such a study, which is planned as future work. Additionally, this paper provides motivation for a trajectory-season optimization study, with initial evidence that strategically scheduling the launches throughout the year has the potential to reduce the sonic boom footprints on land.

VII. CONCLUSION

Rockets launching along the California coast have been producing audible sonic booms on land over 100 km away from the launch site. Evidence from measurements and discussions with local community members suggested that these sonic booms are not observed for every launch and that the likelihood of experiencing one changes throughout the year. This led to the hypothesis that recurring seasonal weather patterns can dramatically affect the sonic boom footprint location.

The goal of this paper was to test this hypothesis and determine dominant meteorological variables. All simulations were performed using a 144° SpaceX Falcon 9 first-stage ascent trajectory in PCBOOM 7.5.0, which was found in this paper to compare favorably with trends observed in measured footprints. Simulations were run using measured and modeled weather profiles from 2020 to 2025. Each stratified atmosphere was used to produce ground footprints. The footprints were then interpolated to four locations in the study area, within the communities of Carpinteria, Ojai, Ventura, and Oxnard.

Strong seasonality was observed at the locations in the study. For all locations, there is a boom "season" lasting primarily from October to April (seven months), where launch trajectories along this 144° heading are substantially more likely to produce high-amplitude sonic booms over a relatively large land area. During the remaining months, from May to September (five months), the launches along this heading produce far fewer sonic booms on land, with the exact amount being location-specific (Fig. 5). It was determined that the seasonal changes in upper-level winds (above 15 km) play a strong role in driving these large seasonal changes in sonic booms on land.

Using these results, it is proposed that SSLS be investigated as a means of reducing the sonic boom footprints on land while still enabling launch providers to launch all their missions each year. This could be implemented by launching coastal trajectories primarily in the summer months (May–September) when they are less likely to produce high-amplitude sonic booms over large land areas. Subsequently, the trajectories that are farther from the coast can be primarily launched during the winter months (October–April) so that the sonic boom footprint on land is reduced. Further studies of different trajectories through different seasons will need to be performed before concrete recommendations can be given, but this paper provides initial insight that this strategy could work.

ACKNOWLEDGMENT

This work was funded by VSFB Space Launch Delta 30, approved for public release, case number 20260402-001. The authors would also like to thank the anonymous reviewers for their time and effort on behalf of this manuscript.

AUTHOR DECLARATIONS

Conflict of Interest

The authors have no conflicts to disclose.

DATA AVAILABILITY

The data that support the findings of this study are available from the corresponding author upon reasonable request. The trajectory data are not available for release.

APPENDIX: MONTHLY RANGE REFERENCE ATMOSPHERES

The monthly range-reference atmospheres were obtained from a 1983 report about Vandenberg Air Force (now Space Force) Base titled "Range Reference Atmosphere 0–70 km

02 November 2026 18:49:36

https://doi.org/10.1121/10.0046863

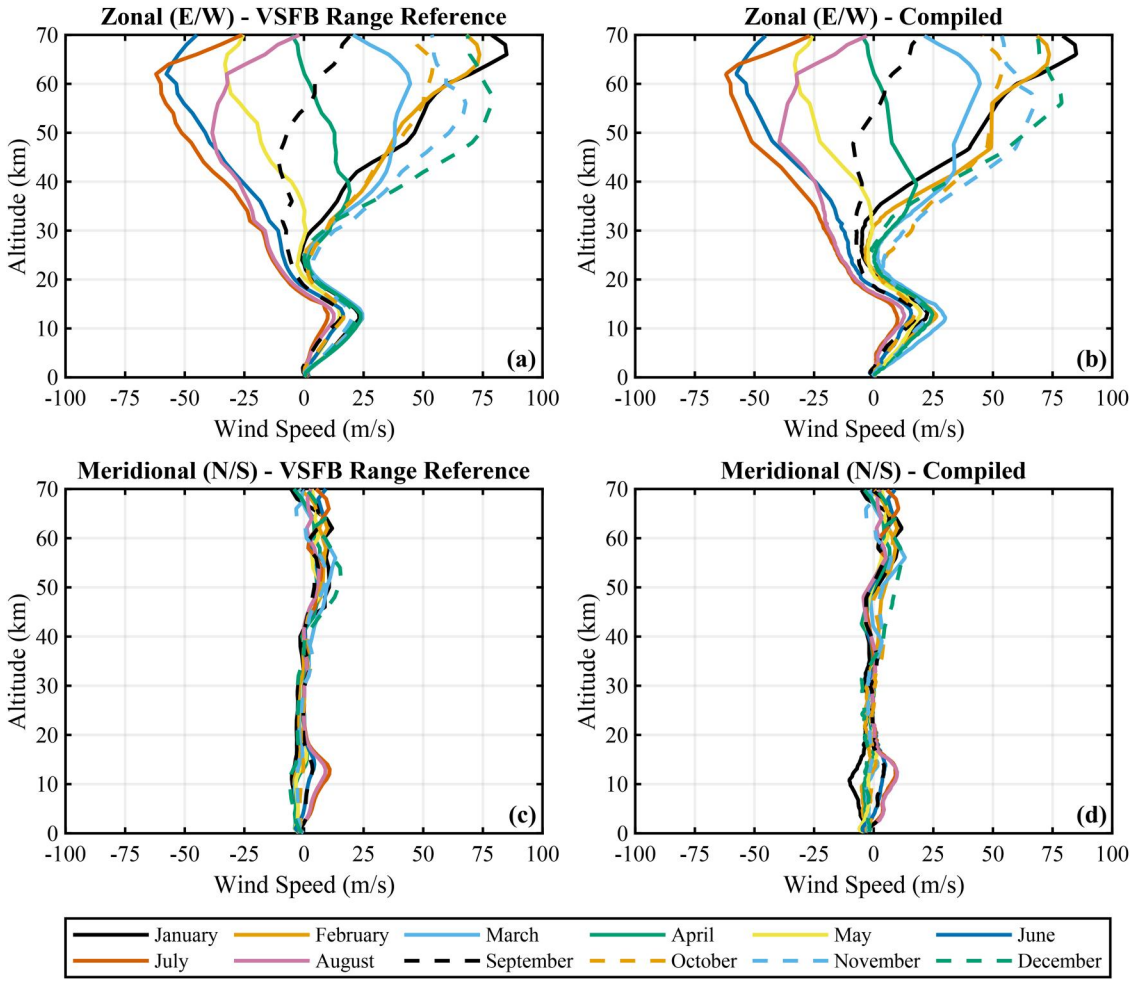


FIG. 9. The monthly range reference atmosphere wind components (Boire *et al.*, 1983) compared with the mean monthly atmosphere wind components using the weather profiles created in this paper. (a) The VSFB range reference atmosphere zonal wind components, (b) the compiled atmosphere zonal components, (c) the VSFB range reference atmosphere meridional components, and (d) the compiled atmosphere meridional components. (a) and (b) A positive number indicates a westerly (eastward blowing) wind component and vice versa, (c) and (d) a positive number indicates a southerly (northward blowing) wind component and vice versa.

Altitude" (Boire *et al.*, 1983). The monthly wind profiles were extracted for use in this paper, whereas the pressure and temperatures were not sufficiently legible, and the relative humidity was not directly available. The wind components are shown in Fig. 9. Although only the top portion (55–70 km) of these wind profiles were used in the analyses in this paper, these profiles are included here to illustrate the seasonal changes in the winds that are discussed throughout this paper. Also shown are the mean monthly wind profiles compiled for this paper from various data sources (see Sec. II B), which show the same trends.

[1]Several of the earliest reports cited in this paper are not publicly available. Citation information often comes from other reports that cite them, and may be incomplete. They are included here to give proper credit and in case any of them become publicly available.

[2]For all checked locations, the final ground signatures are four-point N-waves, and portions of the footprint have four-point signatures with zero overpressure (presumably because the overpressure is modeled to be less than the calculation abilities of PCBOOM). The exception to these results is the focus region, where the signatures are transformed to model propagation through a caustic. Additionally, inspection of the .un6 output files suggest that the starting signature is also an N-wave (albeit with six points, the first two being at $x = 0$ with zero overpressure).

[3]The exception to these details is the relative humidity, which was not available from the IGRA or monthly reference atmospheres, and so comes entirely from the ERA5 simulations. In principle, it could be calculated from other values provided in the IGRA data, but the conversion can become complicated [Lawrence, 2005; World Meteorological Organization (WMO), 2024]. To reduce potential errors in conversion, the ERA5 data are used down to the ground in this analysis. At points higher than the ERA5 simulation data, PCBOOM assumes the highest-altitude value persists to all higher altitudes (Lonzaga *et al.*, 2025b). Because the relative humidity does not affect the ray paths in PCBOOM modeling, these assumptions are assumed to have no impact on footprint locations.

Anderson, M. C., and Gee, K. L. (**2025**). "Modeling seasonal variation in rocket ascent sonic booms," J. Acoust. Soc. Am. **158**, A120.
Bickmore, J., Gee, K. L., Perkins, M., Anderson, M. C., Hall, L. K., and Zepeda, H. (**2025**). "A year's worth of Falcon 9 ascent sonic boom measurements in Southern California," J. Acoust. Soc. Am. **158**, A120.
Bishop, J. W., Blom, P., Carr, C., and Webster, J. (**2025**). "An infrasound source analysis of the OSIRIS-REx sample return capsule hypersonic reentry," J. Acoust. Soc. Am. **158**, 4637–4650.
Boire, G. G., Daniel, O. H., de Violini, R., Finder, F. G., and Fisher, E. E. (**1983**). "Range reference atmosphere, 0-70 km altitude, Vandenberg AFB, California," Technical Report No. 362-83 (National Technical Information Service, Alexandria, VA).
Copernicus Climate Change Service (CCCS) (**2023**). "ERA5 hourly data on pressure levels from 1940 to present," Copernicus Climate Change

02 November 2026 18:49:36

Service (C3S) Climate Data Store (CDS) https://cds.climate.copernicus.eu/datasets/reanalysis-era5-pressure-level-s?tab=overview (Last viewed January 6, 2026).
Downing, J. M., and Plotkin, K. (**1996**). "Validation of launch vehicle sonic boom predictions," J. Acoust. Soc. Am. **100**, 2566.
Drob, D. P., Emmert, J. T., Meriwether, J. W., Makela, J. J., Doornbos, E., Conde, M., Hernandez, G., Noto, J., Zawdie, K. A., McDonald, S. E., Huba, J. D., and Klenzing, J. H. (**2015**). "An update to the Horizontal Wind Model (HWM): The quiet time thermosphere," Earth Space Sci. **2**, 301–319.
Durre, I., Vose, R. S., and Wuertz, D. B. (**2006**). "Overview of the Integrated Global Radiosonde Archive," J. Clim. **19**, 53–68.
Francine, J. K., and Stewart, B. S. (**1995**). "Sonic boom from the Titan IV space launch vehicle launched from Vandenberg Air Force Base," J. Acoust. Soc. Am. **97**, 3258.
Garcia, F. J., Jones, J. H., and Henderson, H. R. (**1983**). "Preliminary sonic boom correlation of predicted and measured levels for STS-5 launch," NASA TM-58253 (NASA, Washington, DC).
Gee, K. L., Kellison, M. S., Anderson, M. C., Moats, L. T., Perkins, M. T., Pulsipher, N. L., Carlston, N. F., Hart, G. W., Hall, L. K., Cantrell, O., Zepeda Villanueva, H. J., McCullah-Boozer, M. R., Budge, R. H., King, J. C., Zering, F. A., Zounes, Z. T., and Mackenthun, K. C. (**2026**). "Falcon 9 ascent sonic boom measurements in Ventura County, California," JASA Express Lett. **6**, 033601.
Glatt, C. R., Hague, D. S., and Reiners, S. J. (**1975**). "Prediction of sonic boom from experimental near-field overpressure data. Volume I: Method and results," NASA CR-2441 (NASA, Washington, DC).
Haber, J. M. (**1981**). "Parametric evaluation of sonic booms resulting from the ascent phase of STS launches from Vandenberg Air Force Base," TR 81-3076-1 (J. H. Wiggins, Co., Redondo Beach, CA).
Henderson, H. R., and Hilton, D. A. (**1974a**). "Sonic-boom ground pressure measurements from the launch and reentry of Apollo 16," NASA TN-D-7606 (NASA, Washington, DC).
Henderson, H. R., and Hilton, D. A. (**1974b**). "Sonic-boom measurements in the focus region during the ascent of Apollo 17," NASA TN-D-7806 (NASA, Washington, DC).
Hersbach, H., Bell, B., Berrisford, P., Biavati, G., Horányi, A., Muñoz Sabater, J., Nicolas, J., Peubey, C., Radu, R., Rozum, I., Schepers, D., Simmons, A., Soci, C., Dee, D., and Thépaut, J.-N. (**2023**). "ERA5 hourly data on pressure levels from 1940 to present," Copernicus Climate Change Service (C3S) Climate Data Store (CDS), https://doi.org/10.24381/cds.bd0915c6 (Last viewed January 6, 2026).
Hilton, D. A., Henderson, H. R., and McKinney, R. (**1972**). "Sonic-boom ground-pressure measurements from Apollo 15," NASA TN-D-6950 (NASA, Washington, DC).
Hilton, D. A., and Henderson, H. R. (**1974**). "Measurements of sonic-boom overpressures from Apollo space vehicles," J. Acoust. Soc. Am. **56**, 323–328.
Kellison, M. S., Gee, K. L., Hall, L. K., Anderson, M. C., Moats, L. T., Perkins, M. T., Pulsipher, N. L., and Hart, G. W. (**2025**). "Falcon-9 ascent sonic boom measurements in Ventura County, California," J. Acoust. Soc. Am. **157**, A62.
Lawrence, M. G. (**2005**). "The relationship between relative humidity and the dewpoint temperature in moist air: A simple conversion and applications," Bull. Am. Meteorol. Soc. **86**(2), 225–234.
Lonzaga, J. B., Page, J. A., Ahearn, M. J., Son, S. R., Downs, R. S., Loubeau, A., and Doebler, W. J. (**2025a**). "PCBoom Version 7.5 User's Guide," NASA TM-20250003188 (Langley Research Center, Hampton, VA).
Lonzaga, J. B., Page, J. A., Downs, R. S., Son, S. R., Ahearn, M. J., Loubeau, A., and Doebler, W. J. (**2025b**). "PCBoom 7 Technical Reference, 2nd edition," NASA TM-20250003228 (Langley Research Center, Hampton, VA).
Loubeau, A., Naka, Y., Cook, B. G., Sparrow, V. W., and Morgenstern, J. M. (**2015**). "A new evaluation of noise metrics for sonic booms using existing data," AIP Conf. Proc. **1685**, 090015.
Loubeau, A., and Page, J. (**2018**). "Human perception of sonic booms from supersonic aircraft," Acoust. Today **14**(3), 23–30.
Lympany, S. V., Salton, A. R., and James, M. M. (**2025**). "Influence of atmospheric variability on sonic boom footprints from rocket launches," J. Acoust. Soc. Am. **158**, A120.
Maglieri, D. J., Bobbitt, P. J., Plotkin, K. J., Shepherd, K. P., Coen, P. G., and Richwine, D. M. (**2014**). "Sonic boom: Six decades of research," NASA SP-2014-622 (Langley Research Center, Hampton, VA).
Maglieri, D. J., Henderson, H. R., Massey, S. J., and Stansbery, E. G. (**2011**). "A compilation of space shuttle sonic boom measurements," NASA CR-2011-217080 (Langley Research Center, Hampton, VA).
Naka, Y. (**2013**). "Subjective evaluation of loudness of sonic booms indoors and outdoors," Acoust. Sci. Tech. **34**, 225–228.
National Oceanic and Atmospheric Administration (NOAA) (**1976**). "U.S. standard atmosphere," Technical Memorandum No. NOAA-S/T-76-1562.
Ortt, J. (**2015**). "A comparison and contrast of environmental monitoring techniques from 2008 to 2014 on the Pacific harbor seal and northern Channel Island pinnipeds," Ph.D. thesis, North Carolina State University Raleigh, NC.
Plotkin, K. J., Franz, R. J., and Haering, E. A., Jr. (**2006**). "Prediction and measurement of a weak sonic boom from an entry vehicle," J. Acoust. Soc. Am. **120**, 3077.
Shepherd, K. P., and Sullivan, B. M. (**1991**). "A loudness calculation procedure applied to shaped sonic booms," NASA TP-3134 (NASA, Washington, DC).
Stanley, J. F. (**1984**). "Sonic boom measurement for space shuttle," J. Acoust. Soc. Am. **76**, S53.
Stansbery, E. G. (**1985**). "An experimental investigation of the Space Shuttle sonic boom," Ph.D. thesis, University of Houston, Houston, TX.
Stansbery, E. G., and Stanley, J. F. (**1984**). "Sonic boom levels measured for STS-41-D launch," NASA JSC-20218 (NASA, Washington, DC).
Stansbery, E. G., Stanley, J. F., and Potter, A. E. (**1983**). "Sonic boom levels measured for STS-7 launch," NASA JSC-19237 (Lyndon B. Johnson Space Center, Houston, TX).
Stewart, B. S. (**1993**). "Behavioral and hearing responses of pinnipeds to rocket launch noise and sonic boom," J. Acoust. Soc. Am. **94**(3_Supp), 1828.
Tiegerman, B. (**1975**). "Sonic booms from drag dominated hypersonic vehicles," Ph.D. thesis, Cornell University, Ithaca, NY.
WMO (**2024**). "Guide to instruments and methods of observation. Volume I—measurement of meteorological variables," https://library.wmo.int/records/item/68695-guide-to-instruments-and-methods-of-observation?offset=2, pp. 197–198 (Last viewed August 10, 2026).
Wooten, R. C. (**1983**). "Space Shuttle Environmental Effects: The First Five Flights," edited by A. E. Potter, NASA CR-171812 JSC-19091 (Lyndon B. Johnson Space Center, Houston, TX).

02 November 2026 18:49:36